Petroleum Res. J. Vol. 16 (2004): P. 1–10, 25 Figs.

Numerical Study of Vortex Shedding from Different Shaped Bluff Bodies

Abubaker Awidat Salem and Yasser Fathi Nassar*

دراسة عددية لظاهرة الدوامات خلف أجسام مختلفة الأشكال

أبو بكر عويدات سالم وياسر فتحي نصار

تم التعامل مع الجريانات المضطربة باستخدام نموذج Baidwi-Lamax وذلك بالاعتماد على برنامج حاسوب متخصص لنماذج الدوامية دالة السريان المشتقة من معادلات Navier-Stokes للجريان اللانضغاطي غير المستقر. كما استخدم البرنامج أيضاً لتحليل السريانات في مقاييس الجريان الدوامية وتحديد أفضل مواصفات الأداء، وتمت مقارنة أرقام Strouhal المحسوبة مع الأرقام التجريبية، حيث أوضحت مجالات السريان أن لشكل الجسم تأثير على حجم وقوة الدوامات المتولدة وكان أكبرها خلف الجسم الأسطواني على هيئة حرف T.

وأعطت الحسابات مؤشراً واضحاً لتكون الدوامات الثانوية قرب جدار المقياس والوجه الأمامي للجسم، هذا بالإضافة إلى تكون الدوامات الابتدائية.

Abstract: *A computer code based on the stream function-vorticity formulation of the unsteady incompressible Navier-Stokes equations has been adapted to treat turbulent flows using the Baidwin-Lamax turbulence model. The code was then used to analyze the flow inside vortex flow meters with the aim of optimizing performance. The computed Strouhal numbers compared well with those acquired experimentally and the computed flow fields indicated how the bluff body shape could influence the size and strength of the shed vortices, with T-shaped cylinder producing the largest vortices. In addition to the primary vortices shed from bluff body, the computations gave a clear indication of the formation of secondary vortices near the meter wall and the front face of the bluff body.*

* Mechanical Engineering Department, University of Sebha, P. 0. Box 53808, Brack, Ash Shati, Libya.
abubakerawidat@hotmail.com

Keywords: vortex shedding; bluff bodies; simulation.

Nomenclature

A+	= 26.0, constant in equation (5)
b	Constant in equation (7)
C_{CP}	= 1.6, constant in equation (8)
C_{KLEP}	= 0.3, constant in equation (11)
C_{WK}	= 0.25, constant in equation (9)
D	Diameter of bluff body
D	Pipe diameter
D_V	Van Driest damping factor
F	Vortex shedding frequency; dominant frequency
$F_{KLEB}(Y)$	Kelebanoff intermittency factor
F_{MAX}	Maximum of function F(Y)
F_{WAKE}	Outer function in equation (10)
K_C	= 0.0 168, Clauser's constant (equations (1)and (8))
K_V	Von Karman's constant (equation (4))
L	Length of vortex shedder in flow direction
Re	Reynolds number
St	Strouhal number

t	Time
T	Dimensionless time
u	Velocity component in x direction
u_τ	Friction velocity
U	Free-stream velocity
V	Velocity component in y direction
X,Y	Cartesian coordinates
Y	Distance from the wall
Y_{max}	Value of Y at which F(Y) (equation (10)) is maximum
δ	Boundary layer thickness
δ^*	Displacement thickness
ν_e	Effective viscosity
ν_l	Laminar viscosity
ν_τ	Turbulent viscosity
X	= 0.4, constant in equation(7)
Ω	Vorticity

INTRODUCTION

The aim of the vortex shedding flow meter manufacture is to produce a device, which efficiently produces strong vortices. This means designing a bluff body, which, with small pressure losses, generates easily detectable vortices whose shedding frequency varies linearly with flow rate over a wide range of Reynolds numbers. Trial and error techniques have been applied widely to perform the development of such meters but they do not necessarily ensure the optimum design of these devices.

New research tools have emerged recently for both experimental and analytical applications. Experimental progress has advanced through Laser Doppler velocimetery, which has been successfully applied to fluid metering research[1,2]. Analytically, computer modeling techniques have been established which might offer an accurate and reliable method for flowmeter improvements[3].

As computer speed and storage capacity have increased in the last two decades, the latter technique has become feasible for handling complex flows, such as unsteady flows, which usually require large amounts of computer time. An early computer simulation of vortex shedding at low Reynolds number was reported by From and Harlow[4]. However, examination of the literature shows that relatively few numerical studies of shedding from bluff bodies have been done. Moreover, most of the work was carried out using a circular cylinder[5] as the vortex shedder, with other bluff bodies receiving much less attention. However, the flow past shedders of rectangular, elliptical and T-shaped cross-section have been studied more recently[6, 7]. Most numerical studies of vortex shedding are performed at fairly low Reynolds numbers in order to exclude the complications by the introductions of a turbulence model. In some of the calculations undertaken, with turbulence modeling, numerical errors might have influenced the results, and, thus, unsatisfactory results are not always attributable to the turbulence model. Here, a turbulence model was added to a laminar computer code[8] in order to study the flow structures around the bluff body at realistic Reynolds numbers.

This paper presents the results of a study designed to extend the laminar computer code[8], based on the stream function-vorticity formulation of the unsteady incompressible Navier- Stokes equation, to treat turbulent flows. The aim is to analyze the flows past the bluff shedder bodies used in many commercial vortex shedding flow meters in order to optimize the bluff body design.

EDDY-VISCOSITY TURBULENCE MODEL

In 1877, Boussineq[9] proposed that the turbulent shear stresses in the momentum equations could be replaced by the product of the mean velocity gradient and a turbulent viscosity ν_τ. The turbulent viscosity was then expressed in terms of auxiliary equations, constructing the turbulence model. In 1925 Prandtl[10] proposed the first turbulence model, which has become known as the mixing-length hypothesis. This model employs an algebraic relation for ν_τ, which is equal to the local product of the magnitude of the mean rate of strain and the square of a characteristic length scale of the turbulent motion.

It is well known that the eddy-viscosity is not constant across a boundary layer, as the turbulence is suppressed close to the wall. Thus, many experiments were performed in order to drive this equation. As a consequence, many algebraic eddy-viscosity models have been produced. One of the most widely used models for the turbulent flow field calculation is that proposed by Cebeci and Smith[11] as double layer turbulence model. This takes the form:

$$(\nu_\tau)_{outer} = K_C U \delta^* [1 + 5.5(Y/\delta)^6]^{-1} \quad (1)$$

where δ is the boundary layer thickness, Y is the normal distance from the wall and K_C is the Clauser constant .This model was then modified[12] by

substituting new relations for conditions at the outer edge of the boundary layer. In particular, the numerical solution was facilitated by eliminating the need to determine the displacement thickness and the boundary layer thickness. This was achieved by introducing two factors, C_{KLEB} and C_{CP}, which were given constant values .The values are discussed later in this section.

In the present investigation, the laminar viscosity v_l in the original laminar program[8] was replaced by:

$$v_e = v_l + v_\tau \tag{2}$$

where v_e is the effective viscosity. The laminar viscosity was assumed constant throughout the present work, while the turbulent viscosity was computed using the Baldwin-Lomax turbulence model[12]. In the Baldwin-Lomax formulation, v_τ is given by:

$$v_\tau = \begin{cases} (v_\tau)_{inner} & Y \le Y_C \\ (v_\tau)_{outer} & Y > Y_C \end{cases} \tag{3}$$

where Y_C is the smallest value of Y at which the values of the viscosity from the inner and outer region formulae are equal. In the inner region, the eddy-viscosity is given by Prandtl-Van Driest formulation:

$$(v_\tau)_{inner} = (K_v Y D_v)^2 \, |\Omega| \tag{4}$$

where K_V is the Von Karman constant and D_V is the Van Driest damping factor, which is given by:

$$D_v = 1 - \exp(-Y / A) \tag{5}$$

where A^+ is a constant and Y^+ is given by:

$$y^+ = \frac{u_\tau}{v_w} \tag{6}$$

where v_w is the kinematic viscosity at the wall and u_τ is the friction velocity. In the present work, v_τ was computed by using Prandtl's velocity distribution law as follows:

$$\frac{u}{u_\tau} = \frac{1}{\chi} \ln Y + b \tag{7}$$

where $\chi = 0.4$ and b are constants. In the outer region, Baldwin and Lomax replaced Clauser's formulation (used by Cebeci and Smith[11]) by the following relation:

$$(v_\tau)_{outer} = K_C \, C_{CP} \, F_{WAKE} \, F_{KLEB}(Y) \tag{8}$$

where C_{CP} is an additional constant. The outer function F_{WAKE} is given by:

$$F_{WAKE} = \text{the smaller of } \left\{ \begin{matrix} Y_{max} F_{max} \\ C_{wk} \, Y_{max} \, u^2_{DIF} / F_{max} \end{matrix} \right\} \tag{9}$$

where C_{WK} is a constant, and F_{MAX} and Y_{MAX} are determined from the function:

$$F(Y) = Y|\Omega|[1 - \exp(-Y^+ / A)] \tag{10}$$

F_{max} is the maximum value that the function F(Y) takes in a local profile , and Y_{MAX} is the value of Y at which F_{max} occurs The function F_{KLEB} (Y) appearing in equation (8) is the Klebanoff intermittency factor, which is given by:

$$F_{KLEB}(Y) = [1 + 5.5 \, (C_{KLEB} \, Y / Y_{max})^6]^{-1} \tag{11}$$

where C_{KLEB} is a constant. The quantity U_{DIF} is the difference between the maximum and minimum total velocity in the profile:

$$u_{DIF} = (\sqrt{u^2 + v^2})_{max} - (\sqrt{u^2 + v^2})_{min} \tag{12}$$

The constants appearing in the above equations were determined by Baldwin and Lomax by requiring the boundary layer profiles computed with the present model to be in agreement with those determined using the Cebeci and Sn jth model mentioned earlier. The values were determined to be:

$A^+ = 26$, $K_V = 0.4$, $K_C = 0.0168$, C_{CP}, $= 1.6$, $C_{KLEB} = 0.3$ and $C_{WK} = 0.25$.

The major difficulty faced here in applying the present model to the calculation of the confined flow past a vortex shedder is to find the correct estimate for Y. This is due to the presence of the shedder walls and as a consequence there is more than one possible Y value. However, the value of Y was computed as the normal to the main flow direction, since this value gave the best results compared with the experimental values.

RESULTS AND DISCUSSION

Using the modified Laminar program and the Baldwin-Lomax turbulence model, the computation

of the flow inside the vortex shedding flowmeter at the bluff body mid-span was performed. This program was also tested with the mixing-length turbulence model but the results are not shown in the present paper due to the poor agreement with the experimental and the current computed values. The parameters involved were the shape of the bluff body and its dimensions, the dimensions of the meter body and the Reynolds number. In order to check the performance of the program together with the turbulence model, all of these parameters were set to the experimental values (detailed in Reference 13), and, therefore, the computed values of Strouhal number are compared with those acquired experimentally for all of the configurations involved. The solution was performed on a uniform (190 x73) mesh, the first number being the number of mesh cells in the x-direction and the second in the y-direction. The computed frequencies are based on the periodic fluctuations of the stream function on the centerline just downstream of the shedder. The frequency was averaged over about five cycles, after allowing the fluctuations to reach a state of approximately constant frequency and amplitude.

The computations of the flow for the vortex meter incorporating a circular cross-section shedder were performed, using the computation grid shown in figure 1. Figure 2 presents a plot of computed instantaneous stream function, 0.055 pipe diameters downstream of the rear face of the shedder, against dimensionless time (T=tU/D) at a Reynolds number (Re = Ud/v) of 9125.

The computed Strouhal numbers (St=fd/U) for various Reynolds numbers are shown together with experimental values in figure 3. For a Reynolds number of 9125, the stream function at T = 10.18 is shown in figure 4. The flow is seen to separate from the bluff body, forming a corrugated wake downstream. This can be seen more clearly in figure 5, which shows the corresponding vorticity contours. There is evidence that a thin contact line is formed between successive vortices, which is the consequence of the entrainment of fluid from one side of the centerline meeting the fluid from the other side. The flow around the rectangular cross-section shedder inside the vortex meter was computed using the computation grid shown in figure 6. The variation of the stream function 0.137 pipe diameters downstream of the rear face of the shedder is shown in figure 7. It is quite clear that the stream function oscillation for this shedder, like that for the circular one, rapidly reaches a reasonably constant amplitude and frequency. The computed Strouhal numbers of various Reynolds numbers are shown, together with the experimental values, in figure 8. For a Reynolds number of 9125, the flow at dimensionless time 11.62 is shown in figure 9 as a stream function plot, and in figure 10 as vorticity contours. In figure 9, the vortices seem to be swept along the rear face of the

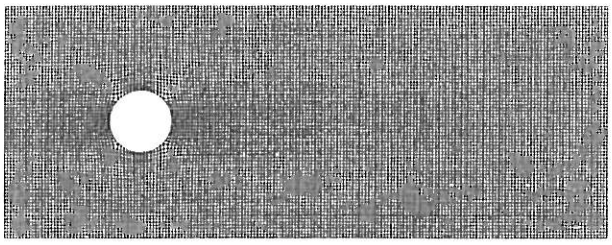

Fig. 1. Computation grid for circular shedder.

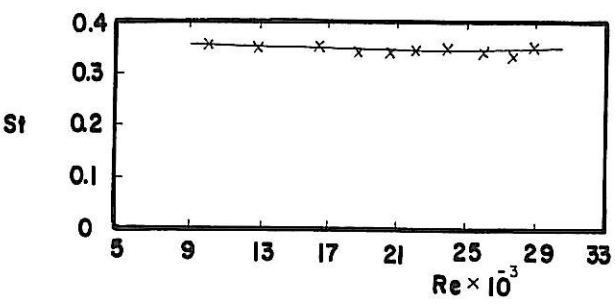

Fig. 3. Strouhal number versus Reynolds number for circular shedder (electrode on splitter plate): x, test meter data; __ , theoretical data.

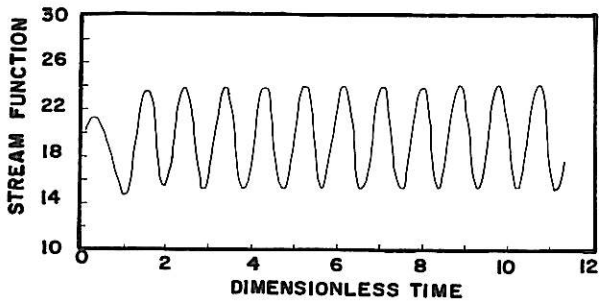

Fig. 2. Instantaneous stream function 0.055 diameters downstream of circular shedder (Re = 912.5).

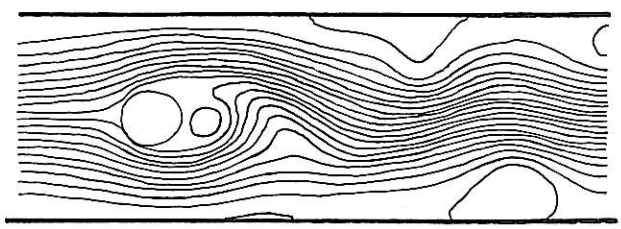

Fig. 4. Flow past circular shedder at T = 10.18 (Re = 9125).

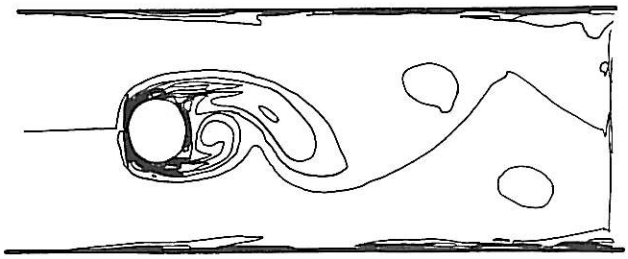

Fig. 5. Vorticity contours for circular shedder.

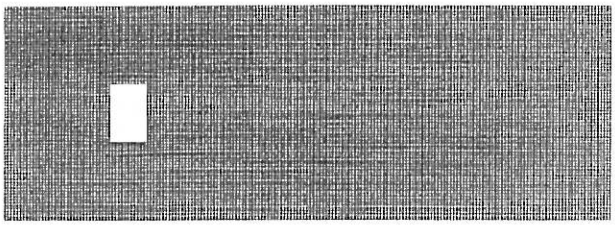

Fig. 6. Computation grid for rectangular shedder.

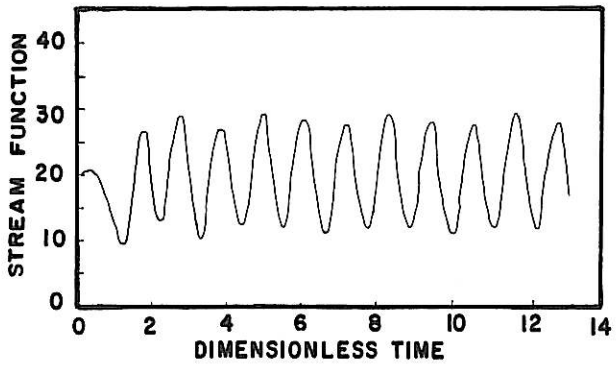

Fig. 7. Instantaneous stream function 0.137 diameters downstream of rectangular shedder (Re = 9124).

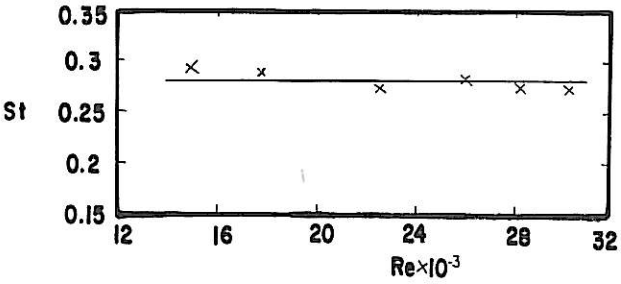

Fig. 8. Strouhal number versus Reynolds number for rectangular shedder (electrode on front face of shedder): x, test meter data ___, theoretical data.

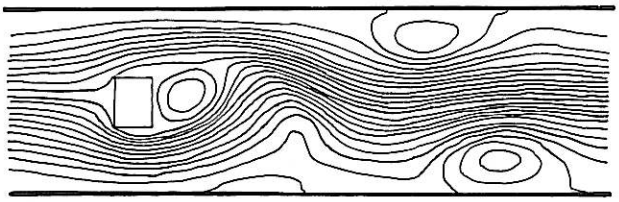

Fig. 9. Flow past rectangular shedder at T = 11.62 (Re = 9125).

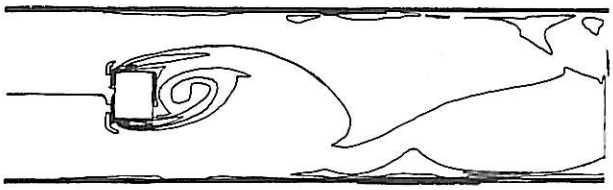

Fig. 10. Vorticity contours for rectangular shedder.

shedder, which is consistent with the other results (see Cousins et al[14]) indicating that the rectangular shedder with L/d close to 0.6 can produce such action, reinforcing the vortex shedding. The vorticity plot (Fig. 10) shows a tendency of the boundary layer to separate from the sharp leading corners of the shedder, and some evidence of reverse flow towards the body surface that is induced by the primary vortices. This plot also shows that small vortices form at both sides of the front face of the shedder. The growth of these vortices was seen to alternate and coincide with the alternating shedding of the primary vortices. These vortices are perhaps responsible for the modulation of the streaming current collected by the electrode attached to the front face of the shedder inside the electrostatic vortex meter [15].

The computation grid (Fig. 11) was used for the calculation of the flow in the vortex meter incorporating a trapezoidal cross-section shedder. The stream function was monitored 0.11 pipe diameters downstream of the rear face of the shedder and its fluctuation is shown (Fig. 12) in which regular vortex shedding is rapidly achieved. The Strouhal number was calculated for a set of Reynolds numbers, which are shown together with the experimental data (Fig. 13). The stream function for a Reynolds number of 9125 is shown in figure 14 at T = 13.0. The corresponding contour of vorticity is shown in figure 15. In this figure, it is quite clear that the vortices do not disappear after their detachment from a teardrop to a more or less circular shape. This action was not apparent for the circular and rectangular cross – section shedders (Figs 5 and 10).

The flow around the triangular cross-section shedder in the vortex meter was calculated using the computation grid shown (Fig. 16). Figure 17 shows the fluctuations of the stream function 0.068 pipe diameters downstream of the bluff body trailing edge. It is clear that, unlike the stream function fluctuations for the previous shedders, the present one exhibits a rather long time to achieve steady state vortex

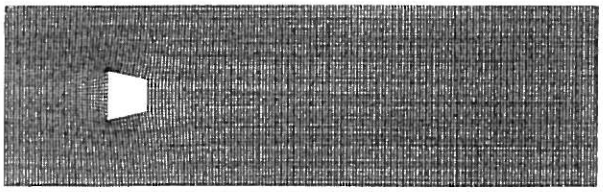

Fig. 11. Computation grid for trapezoidal shedder.

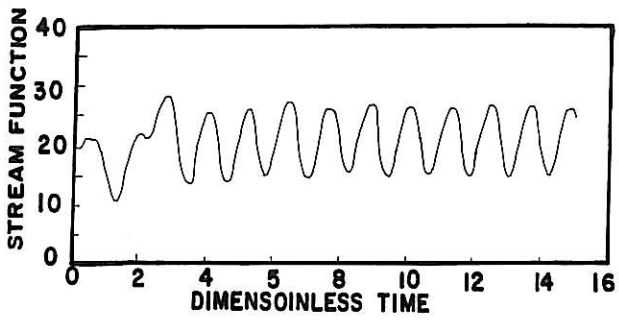

Fig. 12. Instantaneous stream function 0.11 diameters downstream of trapezoidal shedder (Re = 9125).

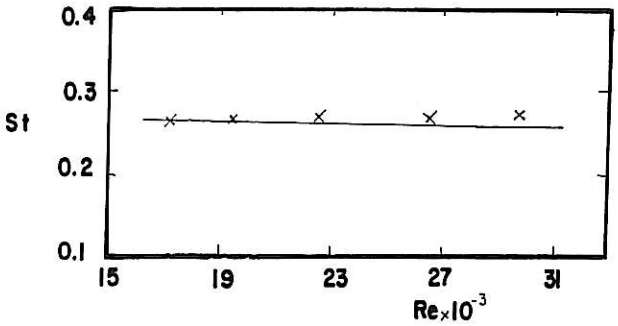

Fig. 13. Strouhal number versus Reynolds number for trapezoidal shedder (electrode on front face of shedder): x, test meter data; __, theoretical data.

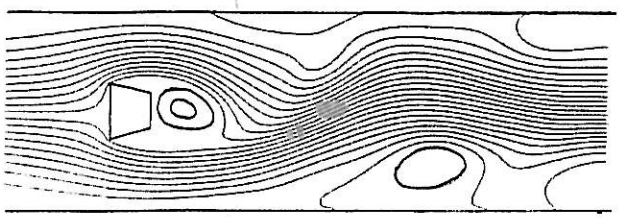

Fig. 14. Flow past trapezoidal shedder at T = 13.0 (Re = 9125).

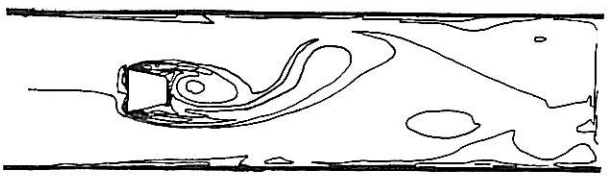

Fig. 15. Vorticity contours for trapezoidal shedder.

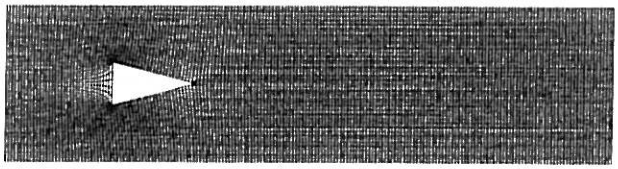

Fig. 16. Computation grid for triangular shedder.

shedding. However, the computed Strouhal numbers (in the regular fluctuation region) for various Reynolds numbers are shown together with experimental values (Fig. 18). It is interesting to monitor the evolution of the flow in the early stages of the calculation. Figure 19 shows illustrative plots for a Reynolds number of 9125. It is clear that at T = 0.16 (Fig. 19a), the flow is approximately symmetrical and in contact with the bluff body sidewalls. The subsequent plot (T = 0.72) reveals the breakup of the symmetrical state when the top recalculation zone moves downward, displacing the bottom recalculation zone. In this figure, it is clear that the vortices are irregular and this may coincide with the large amplitude fluctuations in stream function occurring during the early stages of vortex shedding (Fig. 17). Once the steady-state shedding is reached, the vortices become more regular, like those shown in figure 19c for T = 6.28. The corresponding vorticity contour is shown (Fig. 20).

The flow around a T-shaped shedder in the vortex meter was calculated using the computation grid shown (Fig. 21). Figure 22 shows the fluctuations of the stream function 0.055 pipe diameters downstream of the bluff body trailing edge. Again, the regular fluctuations are rapidly achieved. The Strouhal numbers computed for various Reynolds numbers are shown together with experimental values (Fig. 23).

The stream function at dimensionless time 15.12, for a Reynolds number of 9125, is shown (Fig. 24). Also, the corresponding vorticity contour is shown (Fig. 25). This figure shows that the vortices are larger than those shed by the previous shedders. This may concur with the early finding [16] that the inclusion of a splitter plate into the wake flow from a bluff body renders the separated shear layers thicker and more diffuse. This may highlight the importance of the shedder shape in producing strong vortices, whilst also improving the linearity and the rangeability of the meter incorporating it. This is also in agreement

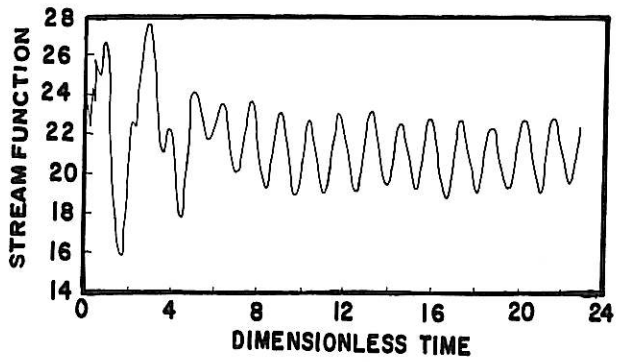

Fig. 17. Instantaneous stream function 0.068 diameters downstream of triangular shedder (Re = 9125).

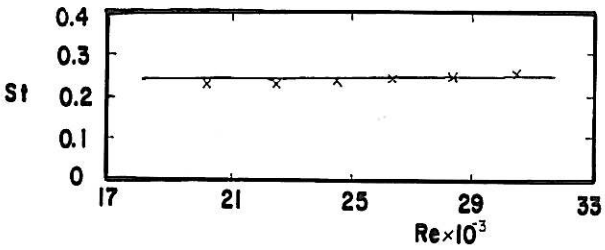

Fig. 18. Strouhal number versus Reynolds number for triangular shedder (electrode on front face of shedder): x, test meter data; __, theoretical data.

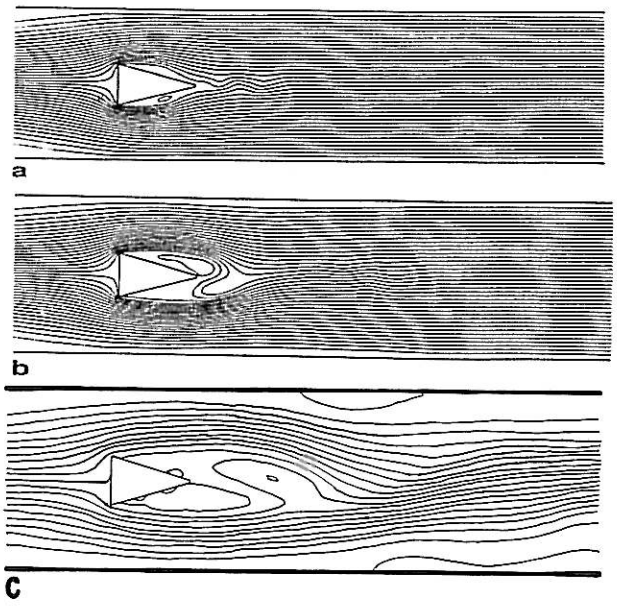

Fig. 19. Flow past triangular shedder (Re = 9125): (a) T = 0.16; (b) T = 0.72; (c) T = 6.28.

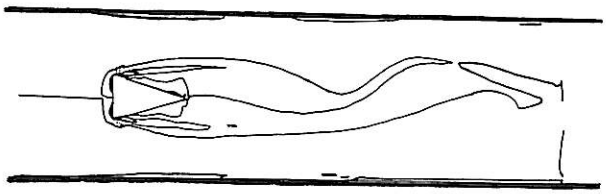

Fig. 20. Vorticity contours for triangular shedder.

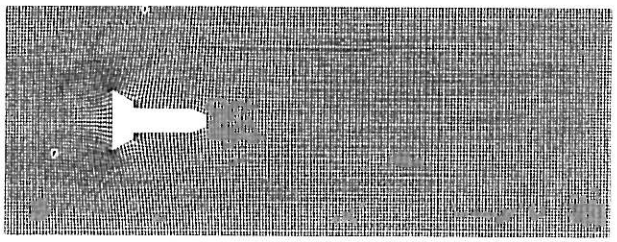

Fig. 21. Comutation grid for T-shaped shedder.

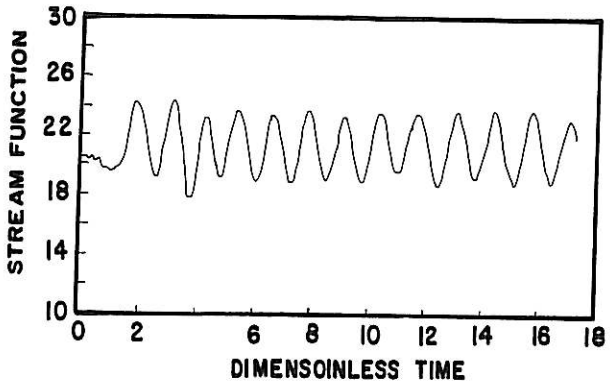

Fig. 22. Instantaneous stream function 0.055 diameters downstream of T-shaped shedder (Re = 9125).

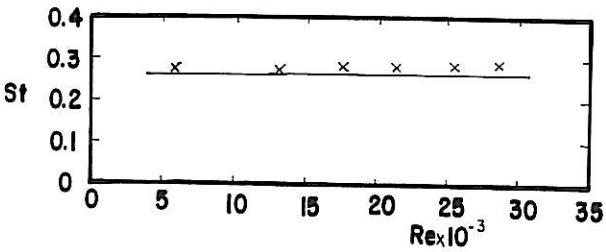

Fig. 23. Strouhal number versus Reynolds number for T-shaped shedder (electrode on front face of shedder): x, test meter data; __, theoretical data.

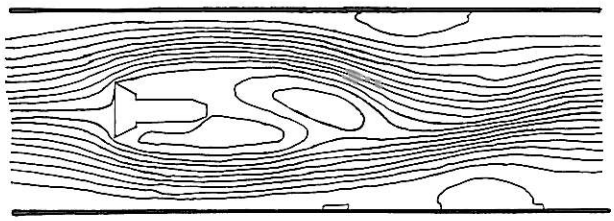

Fig. 24. Flow past T-shaped shedder at T = 15.12 (Re = 9125).

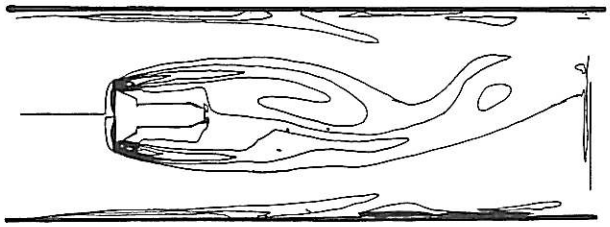

Fig. 25. Vorticity contours for T-shaped shedder.

with the experimental results[13] in which the meter using the T-shaped shedder produced the best signal quality and best meter performance.

For all of the shedders tested, the results indicate that the vortices are concentrated at the centerline of the meter body downstream of the shedder. This may explain the good signal collected by a sensor mounted in this region.

The stream function and vorticity plots reveal that mobile recalculation zones are noticeable on the sidewalls. These wall vortices are formed alternately immediately before the primary vortices collapse. In particular, the pressure at the sidewall decreases to a minimum at a point opposite to the center of the main vortex shed from the bluff body and the pressure downstream of this point increases again. The adverse pressure action seems to encourage the wall vortex to form. This action was noticed experimentally[17] and numerically[6] when this phenomenon was related to the effects of Reynolds number and the blockage ratio d/D. This may explain the rather unexpected performance of the electrode attached to the inner wall of the electrostatic vortex meter downstream of the shedder. Finally, the computed Strouhal numbers compare very well with the experimental data. This may suggest that the computer code together with the turbulence model performed satisfactorily and so can be applied successfully for modeling the unsteady phenomena in other meter types such as the fluidic meter.

CONCLUSIONS

The computer simulation described in this paper was performed in order to examine the flow past the shedder inside a vortex meter. The main points are summarized below:

1. The computed Strouhal numbers are in good agreement with those acquired experimentally. This suggests that the original laminar computer code was successfully extended to handle flow by the addition of the Baldwi-Lomax turbulence model. Accordingly, this model is suitable for modeling separated flows with large recalculation action.

2. The results indicate how the shedder shape can influence the strength of the shed vortices. Among the shedders assessed in this study, the T-shaped shedder produced the largest vortices. This agrees with experimental results in which vortex meters incorporating this shedder gave the best signal quality.

3. There is some indication that small vortices are formed at both sides of the front face of the shedder. These vortices are formed alternately and they are perhaps responsible for the modulation of the steaming current that is collected by the electrode attached to the front face of the shedder inside the electrostatic vortex meter.

4. The vortices seem to be concentrated near the centerline of the meter body behind the shedder. This may explain the good signal collected by a sensor placed in this region.

5. The wall vortices were clearly nearly noticeable in all of the computed flows. These were formed as a result of the adverse pressure gradient on the wall, which is induced by the primary vortices seed from the bluff body. These vortices may also modulate the streaming current collected by the electrode attached to the inner wall of the electrostatic meter.

REFERENCES

[1] Yeh,T. T., Robertson, B. and Mattar, W.M,1983. LDV measurements near a vortex shedding strutcture mounted in a pipe. *J. Fluid Eng., ASME* **105** 185-196.

[2] Nakatani, N., Nishikawa, T., Yoneda, Y. and Yamada, T. 1978. The flow analysis of the vortex shedding flowmeter by the Doppler velocimetery . *Proc . IMEKO, Symp. On Flow Meas.* And *Control in Ind'*. Tokyo 103-108.

[3] Mattingly, G. E.,1985 Prospects for improvements in fluid metering via new esearch tools. *Inter. Conf. On Flow Meas. IMEKO*, Melbourne 1-14.

[4] Fromm, J. E. and Harlow, F. H., 1963. Numerical

solution of the problem of vortex street development. *Phys. Fluid*, **6**, 1976, 975-982.

[5] Jam, P.C. and God, B. S., 1976. Shedding of vortices behind a circular cylinder. *Comput. Fluids,* **4** 137-142.

[6] Davis, R. W., Moore, E. F. and Purtell, L. P. 1984. A numerical experimental study of confined flow around rectangular cylinders. *Phys. Fluids*, **27** (1) 46-59.

[7] Park, j.K., Park, S. O. and Hyun, j. M., Flow regimes of unsteady laminar flow past a slender elliptic cylinder at incidence. *Int. j. Heat Fluid Flow*, **10** (4) 311-317.

[8] Johnson, M. W. 1990. Computation of flow in a vortex-shedding flowmeter. *Flow Meas. Instrum.* **1**(4) 201-208.

[9] Boussinesq, J., 1877. Theorie de l'ecoulement tourbillant. *Mem. Pre. Par.div. Sav.* **23**, Paris.

[10] Prandtl, L., 1925. Bericht uber Untersuchungen zur ausgebildeten Turbulenz. *ZAMM*,**5** (1925), 136. 136.

[11] Cebeci, T. and Smith, A., 1974. *Analysis of Turbulent Boundary Layers* Academic Press, New York.

[12] Baldwin, B. and Lomax, H., 1978. Thin-layer approximation and algebraic model for separated turbulent flows. *AIAA* Paper 78-257 1-8.

[13] El Wahed, A. K., 1991. Electrostatic streaming current and its application to the vortex shedding meter. PhD Thesis, University of Liverpool (1991).

[14] Cousins, T., Foster, S. A. and Johnson, P. A.,1973. A linear and accurate flowmeter using vortex shedding. Inst. Meas. And Control Symp. On Power Fluids for Process Control (1973) 45-56.

[15] Sproston, J. L., El Wahed, A. K. and Johnson, M. W. An electrostatic vortex shedding meter. *Flow Meas. Instrum.* **1**(4) 183-190.

[16] Lucas, G. P. and Turner, j. T., 1985. Influence of cylinder goemetry on the quality of its vortex shedding signal. *Inter Conf. On Flow Meas., IMEKO*, Melbourne (1975) 81-88.

[17] Nagata, H., Kakehi, Y., Tsunekawa, M. and Hasegawa, T., 1975. Unsteady flow past a circular cylinder stared impulsively. *Bull. JSME* **18** (123) 992-1001.